IAI Journals.ASM.org

AMA1-Deficient *Toxoplasma gondii* Parasites Transiently Colonize Mice and Trigger an Innate Immune Response That Leads to Long-Lasting Protective Immunity

Vanessa Lagal,[a,b,c] Márcia Dinis,[a,b,c] Dominique Cannella,[d,e] Daniel Bargieri,[f*] Virginie Gonzalez,[a,b,c] Nicole Andenmatten,[g] Markus Meissner,[g] Isabelle Tardieux[a,b,c]

INSERM U1016, Institut Cochin, Paris, France[a]; CNRS UMR8104, Paris, France[b]; Université Paris Descartes, Sorbonne Paris Cité, Paris, France[c]; CNRS UMR5163, LAPM, Grenoble, France[d]; Université Joseph Fourier, Grenoble, France[e]; Institut Pasteur, Paris, France[f]; Wellcome Trust Centre for Molecular Parasitology, Institute of Infection, Immunity Inflammation, College of Medical, Veterinary and Life Sciences, Glasgow, Lanarkshire, United Kingdom[g]

The apical membrane antigen 1 (AMA1) protein was believed to be essential for the perpetuation of two Apicomplexa parasite genera, *Plasmodium* and *Toxoplasma*, until we genetically engineered viable parasites lacking *AMA1*. The reduction in invasiveness of the *Toxoplasma gondii* RH-AMA1 knockout (RH-AMA1^{KO}) tachyzoite population, *in vitro*, raised key questions about the outcome associated with these tachyzoites once inoculated in the peritoneal cavity of mice. In this study, we used AMNIS technology to simultaneously quantify and image the parasitic process driven by AMA1^{KO} tachyzoites. We report their ability to colonize and multiply in mesothelial cells and in both resident and recruited leukocytes. While the RH-AMA1^{KO} population amplification is rapidly lethal in immunocompromised mice, it is controlled in immunocompetent hosts, where immune cells in combination sense parasites and secrete proinflammatory cytokines. This innate response further leads to a long-lasting status immunoprotective against a secondary challenge by high inocula of the homologous type I or a distinct type II *T. gondii* genotypes. While AMA1 is definitively not an essential protein for tachyzoite entry and multiplication in host cells, it clearly assists the expansion of parasite population *in vivo*.

Toxoplasma gondii certainly belongs to the world champion class of protozoan parasites with a striking ability to colonize most warm-blooded vertebrates worldwide. It is responsible for wildlife and livestock zoonoses with potentially negative socioeconomical impact (1, 2). Remarkably, about a third of the human population is thought to host quasi-silent parasites that persist lifelong after a short-lived and mild primary infection, with a marked tropism for brain and retina tissue reservoirs (3). While the parasitism that proceeds after primary inoculation typically offers lifelong protection to fend off new infections in immunocompetent hosts, immune dysfunction breaks parasite dormancy, promoting uncontrolled expansion of parasites to eventually cause encephalitis and meningitis as major secondary diseases (4).

Despite the fact that there is a wider genetic diversity for parasite genotypes and population structures than previously thought, with 15 current haplogroups differing in frequency and geographic distribution (5), the major lineage that persists and causes damages in human brain is classified as moderately virulent and of the type II genotype. Within the type I strains defined as uniformly virulent in mice, the RH strain, unlike the GT1 genotype, is commonly reported as unable to form persistent cysts in mice (6, 7), although this inability might be the consequence of extensive passages in laboratories (8).

There are, unfortunately, no effective drugs against the cyst-enclosed bradyzoite stage in tissue reservoirs and no vaccines to promote sterile protection against *T. gondii* (9, 10). Live-attenuated strains are among the most efficient ones to confer immune protection: genetic modifications that attenuate the infectious potential of a strain *in vitro* often translate into a short-term infection in mice and a subsequent variable level of immune protection. For instance, *T. gondii* tachyzoites from the RH genotype that were engineered to simultaneously lack the MIC1 and MIC3 microneme proteins had a 100% lethal dose (LD_{100}) in mice of about 2×10^3 parasites whereas the parental strain had an LD_{100} of <20 parasites, and surviving mice were protected against a type II infection (11). This double knockout (KO) (ΔMIC1-3) has shown vaccination efficacy in protection against *T. gondii*-induced abortion in sheep (12). A live-attenuated variant of *T. gondii* was successfully created as an uracil auxotroph (cps) strain which invades cells but does not replicate in the absence of uracil in both healthy and severely immunodeficient mice (13, 14). Interestingly, this safe attenuated strain has shown high potency in promoting tumor regression in mice by reversing tumor-associated immunosuppression when injected in various aggressive tumors (15, 16). However, there is only one licensed vaccine (S48 strain; Toxovax), which is restricted to livestock to reduce miscarriages, congenital

Received 10 September 2014 **Returned for modification** 1 November 2014
Accepted 25 March 2015

Accepted manuscript posted online 6 April 2015

Citation Lagal V, Dinis M, Cannella D, Bargieri D, Gonzalez V, Andenmatten N, Meissner M, Tardieux I. 2015. AMA1-deficient *Toxoplasma gondii* parasites transiently colonize mice and trigger an innate immune response that leads to long-lasting protective immunity. Infect Immun 83:2475–2486. doi:10.1128/IAI.02606-14.

Editor: J. H. Adams

Address correspondence to Isabelle Tardieux, isabelle.tardieux@inserm.fr.

* Present address: Daniel Bargieri, Institute of Biomedical Sciences, University of São Paulo, São Paulo, Brazil.

Supplemental material for this article may be found at http://dx.doi.org/10.1128/IAI.02606-14.

doi:10.1128/IAI.02606-14

toxoplasmosis, and cyst burden in skeletal muscles used for human consumption (17). While the noncystogenic type I RH strain is of primary relevance for live-attenuated vaccines, this strain is in addition routinely amenable to gene disruption, and therefore numbers of "attenuated" phenotypes that relate to parasite motile, invasive, or replicative properties can be reliably revealed by *in vitro* analysis. Finally, the intraperitoneal (i.p.) delivery of either type I or type II tachyzoites triggers quantitatively and qualitatively similar changes in the transcription profiles of the peritoneal cells, therefore validating type I as a reliable model for assessing the early mouse immune response to *T. gondii* (18).

We have recently engineered clones from the virulent *T. gondii* type I RH genotype that lack the apical membrane antigen 1 (AMA1)-encoding gene by applying the diCre-recombinase site-specific recombination strategy (19). AMA1 is a protein stored in secretory vesicles called micronemes and is exposed as a transmembrane protein over the entire parasite surface following polarized secretion at the apex (20). While AMA1-deficient ($AMA1^-$) tachyzoites glide, egress, and replicate normally, they display a significant defect in host cell invasion that decreases invasion efficiency *in vitro* by 2- to 3-fold compared to $AMA1^+$ parasites (19).

To further assess whether AMA1 loss in the *T. gondii* RH strain would impact the ability of the parasite to colonize cells *in vivo*, we applied ImageStream AMNIS technology to simultaneously image and quantify the AMA1 knockout ($AMA1^{KO}$) tachyzoites in mice following i.p. inoculation. The AMNIS approach has already proved valuable to point toward a critical role of infected cells in initiating *T. gondii*-specific $CD4^+$ and $CD8^+$ T cell responses (21).

We document that $AMA1^{KO}$ tachyzoites are capable of invading and multiplying within distinct resident cell lineages, in particular, in the mesothelium as well as within homing cell lineages, although the population expansion remains transient. The rapidly triggered moderately short-term proinflammatory process accounts for the rapid control of the size of the $AMA1^{KO}$ population and its clearance from all the leukocytes in the peritoneal cavity, a process that no longer operates in immunocompromised mice. We therefore conclude that, *in vivo*, AMA1 increased the virulence of the strain by promoting an overall invasiveness of tachyzoites that translated into a rapid expansion of the parasite population. In line with previous studies performed using attenuated virulence strains, we also found that the mice parasitized with $AMA1^{KO}$ were vaccinated against infection even after 8 months postimmunization and against a high inoculum of homologous type I virulent tachyzoites whereas they were partially protected against infection with a type II cystogenic strain (22).

MATERIALS AND METHODS

Reagents and mouse and *T. gondii* strains. Unless otherwise specified, most reagents, including antibodies (Ab), were purchased from Sigma-Aldrich (Saint-Quentin Fallavier, France), while Alexa Fluor secondary antibodies were obtained from Molecular Probes (Life Technologies, St. Aubin, France) and DyLight secondary antibodies from Thermo Scientific (Courtaboeuf, France). For flow cytometry and ImageStream analysis, the Fc blocking antibodies (clone 2.4G2) and the anti-Ly6G antibody (clone 1A8-Brilliant violet 421) were purchased from BD Pharmagen (Le Pont de Claix, France) and the F4/80-phycoerythrin (PE) antibody from Affymetrix eBioscience SAS (Paris, France), while the anti-Ly6C/6G antibody (clone RB6-8C5; Alexa Fluor 547 or 568) was obtained from AbD Serotec (Colmar, France). BALB/cByJ, C57BL/6J, and CD1 IGS female mice (8 to 12 weeks old) were obtained from Charles River Laboratory (l'Arbresle, France). The type I *T. gondii* tachyzoites were of the RHΔ*hxgprt*/Δ*ku80*::*diCre* (23) and RHΔ*hxgprt*/*gfp* genotypes; the type II *T. gondii* tachyzoites were of the ME49 and PruΔ*hxgprt*/Δ*ku80* genotypes (22). Live tachyzoites were collected and purified from synchronously culturing parasites in mycoplasma-free human foreskin fibroblast (HFF) cell monolayers (24).

Ethics statement. This study was performed in strict accordance with the recommendations in the Guide for the Care and Use of Laboratory Animals of the University of Paris Descartes (committee no. 34). The protocol was approved by the Committee on the Ethics of Animal Experiments of the University of Paris Descartes (permit B75-14-11). All surgery was performed using sodium pentobarbital anesthesia, and every effort was made to minimize suffering.

Mouse survival assays. Viable parasites (2.5×10^2 to 10^6) were injected i.p. or subcutaneously into mice in a 100-μl volume of phosphate-buffered saline (PBS). For challenge experiments, naive and $AMA1^{KO}$-injected mice received an i.p. injection of 10^3 (C57BL/6J) or 10^5 (BALB/c, CD-1) $AMA1^+$ parasites 6.5 to 15 weeks after the first injection. *T. gondii* strains used in challenge assays also included the type II ME49 strain, for which 10^3 tachyzoites were injected in BALB/c mice that had been inoculated with 10^5 $AMA1^{KO}$ tachyzoites 8 weeks earlier. In some experiments, 10^5 $AMA1^{KO}$ parasites were injected i.p. into BALB/c mice immunosuppressed with the glucocorticoid dexamethasone (25) during the 2 weeks preceding the inoculation and thereafter (1 mg/mouse every 2 days delivered i.p.). In all assays, mouse survival was monitored daily over a period of 1.5 to 3 months.

Peritoneal fluid harvest and ELISA measurement of cytokine levels. At days 1, 3, and 5 postinoculation (p.i.), peritoneal fluids from mice inoculated with warmed PBS, 10^5 $AMA1^+$, $AMA1^{FLAG}$, and $AMA1^{KO}$ tachyzoites were collected in 1 ml PBS using gentle massage of the peritoneal cavity. Cells were pelleted and pooled with 1 additional wash of the cavity, and they were immediately treated for flow cytometry and ImageStream analysis as described below. The 1-ml supernatant fractions were divided into aliquots and stored at −80°C until use. Concentrations of interleukin-6 (IL-6), CCL2 (also called monocyte chemoattractant protein-1 [MCP-1]), IL-12p70, tumor necrosis factor alpha (TNF-α), and IL-10 chemokines and cytokines were measured in triplicate for each mouse (DuoSet enzyme-linked immunosorbent assay [ELISA] kit; R&D Systems, Lille, France).

Preparation of peritoneal mesothelial cells. After careful removal of the peritoneal fluids (see above), the mesothelial cells were selectively dissociated from the wall according to a protocol which includes *in situ* protease digestion (26). The collected mesothelium-constituting cells were plated and cultured on gelatin (0.1% in PBS)-coated glass coverslips for 3 to 5 h prior to immunofluorescence assays (IFA).

Imaging of immune cells in the peritoneal cavity using ImageStream analysis. After harvest, the peritoneal cells were incubated on ice with Fc blocking antibodies (2.4G2, 5 μg/ml) and subsequently with anti-Ly6G antibodies (1/200 dilution), with anti F4/80-PE antibodies (1/200 dilution,) and with anti-Ly6GLy6C antibodies (1/300 dilution) (4°C, 20 min). A total of 10,000 to 35,000 events were recorded using ImageStream AMNIS technology and excitation lasers with λ values of 405, 488, and 658 nm and analyzed with the IDEAS software from AMNIS.

Viability of parasites assessed by plaque assay. Cells (10^5 and 10^6) collected from the peritoneal fluids were deposited onto a HFF cell monolayer cultured in a 6-well plate. After Giemsa staining, plaques were visualized under an Axiovert II microscope using a 40× objective (Zeiss, Marly-le-Roi, France). Alternatively, time for complete lysis of the monolayer was recorded.

WB analysis, IFA, and confocal microscopy. For Western blot (WB) analysis, whole-cell extracts from 10^6 $AMA1^+$, $AMA1^{KO}$, and $AMA1^{FLAG}$ parasites were analyzed by SDS-PAGE and Western blotting using monoclonal Ab (MAb) B3.90 (20) (1/5,000 dilution) and anti-FLAG antibody (clone M2; 1/4,000 dilution). The M2AP protein was used as an internal

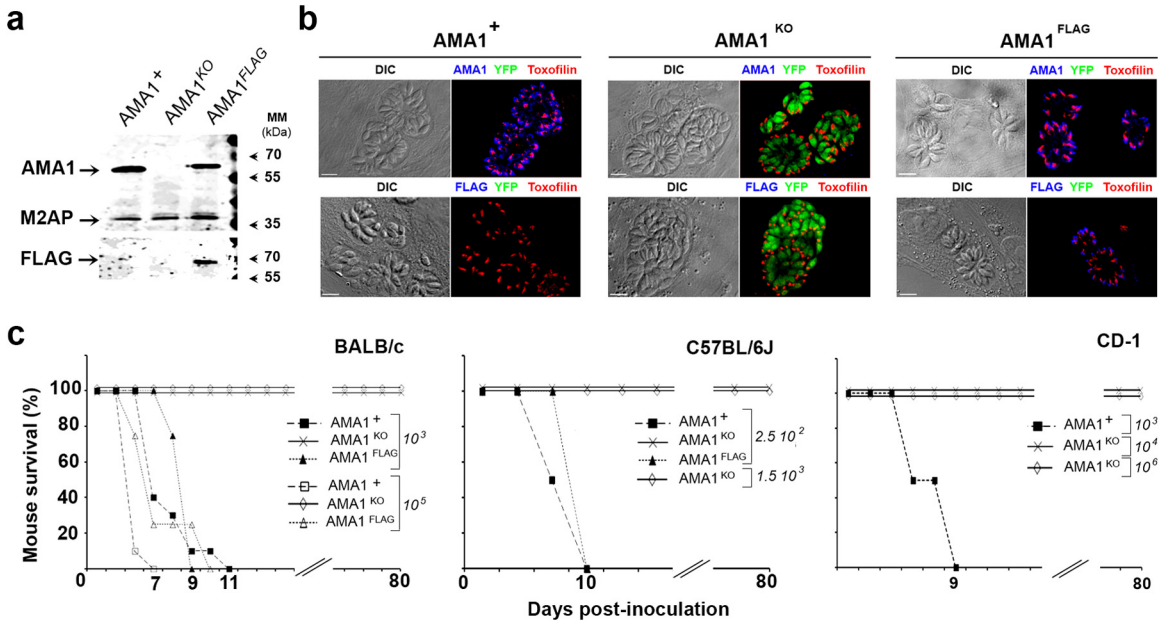

FIG 1 Reduced virulence of the AMA1^{KO} parasites in mice. (a and b) AMA1 protein expression detected in whole-cell extracts of AMA1^{+}, AMA1^{KO}, and AMA1^{FLAG} parasites using anti-AMA1 (top panel) and anti-FLAG (bottom panel) antibodies (M2AP micronemal protein served as a loading control) (a) and in tachyzoites in host cells (differential inference contrast [DIC] [left] and fluorescent [right] images are shown [AMA1 and AMA1^{FLAG}, blue; toxofilin protein, red]) (b). MM, molecular mass. (c) Mouse survival curves for BALB/c, C57BL/6J, and CD-1 mice injected i.p. with different doses of AMA1^{KO} or AMA1^{+} or AMA1^{FLAG} tachyzoites. Bars, 10 μm.

loading control and detected with polyclonal anti-M2AP antibody (27) (1/5,000 dilution). Appropriate secondary DyLight 680 or 800 antibodies were used at a 1/10,000 dilution. Blots were scanned with an Odyssey Infrared Imaging System (Li-COR Biosciences, Courtaboeuf, France), and images were processed with ImageJ software (28).

For IFA, parasites growing in HFF cells for 24 to 32 h were stained with B3.90 anti-AMA1 (19) and anti-toxofilin (29) antibodies after fixation with paraformaldehyde (PFA) (2% in PBS). Peritoneal cells were fixed and subjected to Triton X-100 permeabilization before being incubated with anti-GRA3 antibodies (1/300 dilution) and with anti-F4/80-PE antibodies (1/100 dilution). Some samples were postfixed in cold 100% methanol (1 min) before being stained with anti-cytokeratin (CK) (panCytokeratin; clone C11) (1/200 dilution) or with anti-vimentin (Vim) (clone V9; Santa Cruz Biotechnology, Heidelberg, Germany) (1/150 dilution) antibodies. Appropriate Alexa Fluor 568- or 660-coupled secondary antibodies were used at a 1/1,000 dilution. Samples were analyzed under a confocal microscope (Eclipse T*i*; Nikon, Champigny sur Marne, France). Images were acquired with a CoolSNAP HQ camera (Roper Scientific, Lisses, France) with Metamorph software (Universal Imaging Corporation) and processed with ImageJ and Photoshop software.

Serology control for anti-*Toxoplasma* antibodies. Blood from AMA1^{KO}-inoculated mice was collected from the jugular vein, and sera were separated from the blood clot by centrifugation (2,000 × *g*, 10 min). Seroconversion was checked by SDS-PAGE and Western blot analysis probing whole extracts from 10^6 extracellular tachyzoites with mouse serum (1/10 dilution) and secondary DyLight 680 or 800 antibodies as described above.

Detection of brain cysts and parasite reactivation. Brains from C57B/6J mice surviving at inoculated doses of 2.5×10^2 and 1.5×10^3 AMA1^{KO} parasites were collected 15 weeks p.i. DNA was purified from one half of a mouse brain using TRIzol LS reagent (Life Technologies, St. Aubin, France), while the other half was controlled for cyst by microscope analysis. Parasite genomic DNA was detected by PCR or quantitative real-time PCR (RT-PCR) using specific primers (30) (Tox9 to Tox11), while DNA from brain of C57B/6J mice inoculated 15 weeks earlier with type II Pru:Δ*ku80* parasites served as controls (1 experiment, $n = 3$ mice per strain). For BALB/c mice inoculated 15 weeks earlier with 10^5 or 10^6 AMA1^{KO} parasites, indirect detection of cysts was obtained by treating the mice with dexamethasone every 2 days over 1 month. Mice were monitored daily for sign of *Toxoplasma*-related diseases during 1 month. In challenge assays with the type II strain, BALB/c mice inoculated with 10^5 AMA1^{KO} parasites 8 weeks earlier and naive mice were challenged with 10^3 ME49 tachyzoites. Protection was evaluated 6 weeks postchallenge by microscopic examination of brain homogenates from one half of a brain and by quantification of parasite transcripts by quantitative PCR (qPCR) as described in reference 31.

Statistical analysis. Statistical analyses were performed using Prism Graphpad software. The two-tailed Student's *t* test was applied to all data, and the results were classified as nonsignificant (*NS*) for *P* values of >0.05 and as significant (*), highly significant (**), and very highly significant (***) for *P* values of <0.05, <0.01, and <0.001, respectively.

RESULTS

Mice resist high doses of type I AMA1^{KO} tachyzoites. We have previously demonstrated that a lack of AMA1 results in about a 50% loss in population invasiveness *in vitro*. To assess whether this phenotype could impact parasite fitness *in vivo*, we inoculated BALB/c mice i.p. with different doses of type I tachyzoites (RHΔ*hxgprt*:Δ*ku80*::*diCre* strain) expressing either endogenous AMA1 (DiCre-AMA1^{+} = AMA1^{+}) or an AMA1-FLAG fusion as a replacement for AMA1 (DiCre-AMA1^{FLAG} = AMA1^{FLAG}) or yellow fluorescent protein (YFP) instead of AMA1 (DiCre-YFP^{+}-AMA1^{KO} = AMA1^{KO}) (23) (Fig. 1a and b), and we monitored survival over a period of a minimum of 2 months. In 3 separate experiments ($n = 5$ mice per assay per strain), mice injected with 10^3 and 10^5 AMA1^{+} parasites died within 11 and 7 days postinoculation (p.i.), respectively, whereas all those inoculated with AMA1^{KO} parasites survived (Fig. 1c, left panel). Of note, mice

infected with 10^6 AMA1^{KO} parasites survived but a few showed transient signs of mild pathology (one experiment, $n = 5$ mice per strain, data not shown). Additionally, we used C57BL/6J mice, reported to be more susceptible to different clonal strains of *T. gondii*. While inoculation of 2.5×10^2 AMA1$^+$ parasites was enough to kill C57BL/6J mice within 10 days (one experiment, $n = 5$ mice), these mice survived challenge with 2.5×10^2 and 1.5×10^3 AMA1^{KO} injected parasites ($n = 5$ mice per dose) (Fig. 1c, central panel). Finally, the robust outbred CD-1 mice (32) resisted challenge with 10^4 to 10^6 AMA1^{KO} tachyzoites whereas they succumbed within 9 days when injected with 10^3 AMA1$^+$ tachyzoites (one experiment, $n = 4$ mice per dose) (Fig. 1c, right panel). Similar survival phenotypes were observed when 10^3 and 10^5 AMA1^{KO} tachyzoites were administered subcutaneously to BALB/c mice, while 10^3 AMA1$^+$ parasites killed mice within 11 days (one experiment, $n = 4$ mice; see Fig. S1a in the supplemental material). Importantly, reintroduction of a FLAG-tagged copy of AMA1 into the AMA1^{KO} strain (Fig. 1a and b) that restored the parental invasiveness *in vitro* reestablished the lethal phenotype in both BALB/c and C57BL/6J mouse strains following i.p. delivery (Fig. 1c, left and central panels), thereby suggesting that AMA1 acts as a novel important virulence determinant *in vivo*.

AMA1^{KO} tachyzoites induce a short-term proinflammatory response following intraperitoneal inoculation. Parasite delivery in the peritoneal cavity of mice typically activates leukocytes and nonleukocytic cells to rapidly produce chemokines, in particular, the chemotactic CCL2 (also called MCP-1) protein that drives an influx of Gr1$^+$ inflammatory monocytes (33). These monocytes promote gamma interferon (IFN-γ) synthesis by producing interleukin-12 (IL-12) and tumor necrosis factor alpha (TNF-α) and are critical to elicit an efficient innate response during infection by a type II persistent strain (34–36). In the case of type I strains, tachyzoites largely gain their virulence by escaping the IFN-γ-dependent IRG (immunity-related guanosine triphosphatase) killing activity and the subsequent clearance of infected host cells (37). The essential virulence factors responsible for this activity are now well identified as members of the polymorphic rhoptry-secreted kinase family (ROPs) that work in a combined way to avoid the IRG recruitment to the parasite-containing vacuoles (38). The resulting uncontrolled burst of the tachyzoite population, together with activation of macrophages and dendritic and NK cells and the deleterious effects of neutrophils at the inflamed tissues, eventually causes animal death (35, 36).

We characterized the cytokine/chemokine profiles in the peritoneal exudates of BALB/c mice inoculated with PBS or with 10^5 parasites from AMA1-expressing strains (AMA1$^+$ and AMA1^{FLAG}) or from the AMA1^{KO} strain at different time points p.i. (1 mouse each for PBS and AMA1^{FLAG} and 2 to 3 mice for both AMA1$^+$ and AMA1^{KO} at each time point; one experiment representative of three experiments) using ELISA. Comparing the results to those seen with the PBS control injection, we found a high increase in IL-6 secretion by mice inoculated with AMA1-expressing tachyzoites that exceeded 2,800-fold at day 3 p.i. and reached 1,490-fold at day 5 p.i. whereas it rose to only 335-fold in mice inoculated with AMA1^{KO} tachyzoites at day 3 p.i. and declined quickly at day 5 p.i. (Fig. 2a, left histogram). The rapid induction of CCL2 following injection of parasites was also more pronounced in mice inoculated with AMA1-expressing strains, but the differences between these mice and those injected with AMA1^{KO} tachyzoites were only 2.4-fold and 3.7-fold at days 1 and 3 p.i., respectively (Fig. 2a, central histogram). Interestingly, substantial levels of IL-12 secretion (measured using IL-12p70), which are usually associated with type II strain infection, were rapidly detected 1 day p.i. and remained within the same range of increase in mice inoculated with tachyzoites expressing or lacking AMA1 (300-fold or 200-fold, respectively), decreasing thereafter to almost the control level at day 5 p.i. (Fig. 2a, right histogram). Finally, while TNF-α was barely detectable in any of the mice analyzed, the counterinflammatory IL-10 cytokine known to downregulate IL-12 production was detected only weakly in AMA1$^+$-infected mice and remained undetectable upon injection of AMA1^{KO} tachyzoites (data not shown). Therefore, the relatively minimally inflammatory process observed following i.p. injection of AMA1^{KO} tachyzoites was unlikely to have resulted from counteracting anti-inflammatory activities.

In addition, the extent of proinflammatory cytokine/chemokine secretion in response to AMA1-expressing or AMA1^{KO} tachyzoite injection concurred with increasing amounts of cells harvested in the peritoneal cavity: compared to PBS injection, an increase of about 2.5-fold was observed as early as 1 day p.i., regardless of the parasite inoculum (Fig. 2b, 1 representative experiment of 3 separate assays, triplicate). However, the amount of cells rose with time only slightly in mice that were injected with AMA1^{KO} tachyzoites whereas the increase rapidly exceeded 10-fold in mice inoculated with either AMA1$^+$ or AMA1^{FLAG} tachyzoites (Fig. 2b). Collectively, these data demonstrate that the loss of AMA1 significantly impacts the parasite-driven immunological process(es) in mice. More specifically, the parasite population lacking AMA1 induces a moderate and short-term proinflammatory early innate response involving IL-6, CCL2, and IL-12 secretion, which associates with a modest recruitment of immune cells compared to the levels seen with the wild-type and complemented parasite populations.

AMA1^{KO} tachyzoites colonize resident and recruite leukocytes in the peritoneal cavity after inoculation. We next verified whether AMA1-lacking parasites could parasitize the cells homing in the peritoneal cavity in response to inoculation. First, a fraction of the peritoneal cells collected at different times p.i. was observed *in situ* after these had spread on a gelatin substrate and following immunostaining of the dense granule (GRA3) tachyzoite protein. This label was used as a proof of tachyzoite multiplication, since GRA3 is secreted into the parasitophorous vacuolar (PV) space and associates with the parasitophorous vacuolar membrane (PVM) during intracellular growth (Fig. 3a, white arrowheads) (39). In addition, mutant but not wild-type tachyzoites were detected by green fluorescence because the YFP-encoding sequence is inserted at the *AMA1* locus in the RH-AMA1^{KO} genome (see Fig. 1a and b). Qualitative cell analysis of peritoneal exudates from mice inoculated with either AMA1$^+$ or AMA1^{KO} tachyzoites revealed PVs containing up to 2 parasites as early as 7 h p.i. and PVs enclosing between 1 and >8 tachyzoites at 32 to 35 and 72 h p.i. (Fig. 3a). These observations attest that both parasite populations had undergone several rounds of replication, and, as expected, the higher AMA1^{KO} tachyzoite inoculum resulted in larger initial amounts of infected cells (Fig. 3a, right panel, white arrows, and data not shown).

We then simultaneously identified and imaged peritoneal cells

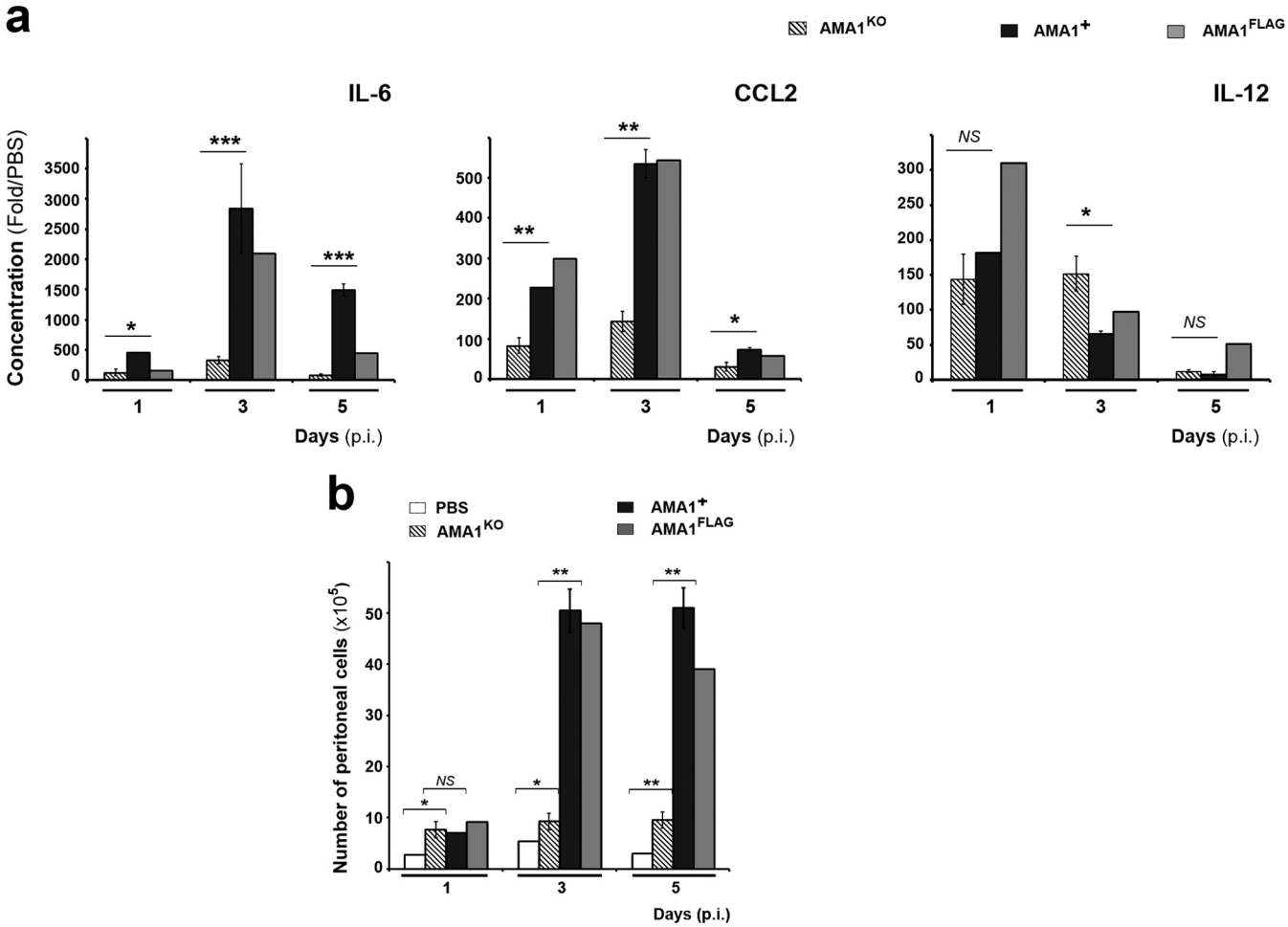

FIG 2 AMA1^{KO} tachyzoites induce a moderate proinflammatory cytokine response. (a) IL-6, CCL2, and IL-12 cytokine concentrations in the peritoneal cavity of mice inoculated with PBS, AMA1^{KO}, AMA1^{+}, and AMA1^{FLAG} at days 1, 3, and 5 p.i. Data represent the results of one experiment representative of three independent assays and are expressed in severalfold values with PBS as a reference. (b) Fluorescence-activated cell sorter (FACS) enumeration of cells collected in the peritoneal exudates at days 1, 3, and 5 p.i. Data represent mean values ± standard errors of the means (SEM) of the results of 1 assay representative of 3.

in mice inoculated with parasites expressing or not expressing AMA1, using the ImageStream AMNIS technology. To detect cells that hosted parasites, we used RH green fluorescent protein (GFP^{+})-AMA1^{+} (= GFP^{+}-AMA1^{+}) tachyzoites as controls because they are fluorescent and their survival rate in mice was previously described as being of the same range as that seen with the RHΔ*hxgprt*:Δ*ku80*::*diCre* strain (8). Nonimmune cells and tissue-resident macrophages as well as inflammatory monocytes and neutrophils were recognized using combinatory sets of antibodies directed against surface proteins that commonly served as cell subset markers (see Materials and Methods). Analysis of 11,000 to 35,000 peritoneal cells for each mouse and time point ($n = 2$ mice per time point except for PBS results analyzed at day 1 p.i. only and with $n = 2$ mice in 2 separate assays) revealed that the F4/80^{-} Ly6C/6G^{+} population constituted the dominant inflowing population within 3 days post-tachyzoite inoculation and that the results were independent of AMA1 expression (Fig. 3b). As expected, we also observed a transient recruitment of F4/80^{+} Ly6C/6G^{+} cells, likely Gr1^{+} inflammatory monocytes, in particular, for the AMA1^{KO}-inoculated mice, that peaked between days 3 and 4 p.i. and declined further (Fig. 3b). The reduction in Gr1^{+} inflammatory monocytes correlated with a relative increase in the numbers of F4/80^{+} Ly6C/6G^{-} macrophages, an observation consistent with the reported capacity of the former to differentiate into macrophages (40).

Regarding the rate of infection, data analysis showed a rapidly occurring gap between the two parasite populations in the numbers of parasite-positive cells. They scored at 4.2% and 59.2% of total cells for AMA1^{KO} and AMA1^{+} 4 days p.i., respectively, and these rates decreased thereafter for the former population whereas they continued to rise for the latter (Fig. 3c; data are given for 1 experiment representative of 2, $n = 2$ mice for each time point). At this maximal rate of infection, AMA1^{KO} tachyzoites were predominantly (53.45%) observed in F4/80^{+} Ly6C/6G^{+} inflammatory monocytes (Fig. 3d, day 4). In addition, F4/80^{+} Ly6C/6G^{-} leukocytes, which represented the resident macrophage subpopulation, accounted for 6% of the infected peritoneal cells and the remaining 28.5% cells were detected as F4/80^{-} and Ly6C/6G^{+}. At a later time (i.e., day 5 p.i.), the proportion of resident macrophages hosting AMA1^{KO} tachyzoites markedly increased (up to 56.4%; see Fig. 3d), although this cell subset represented about 20% of the collected peritoneal cells (Fig. 3c). Furthermore, when the in-

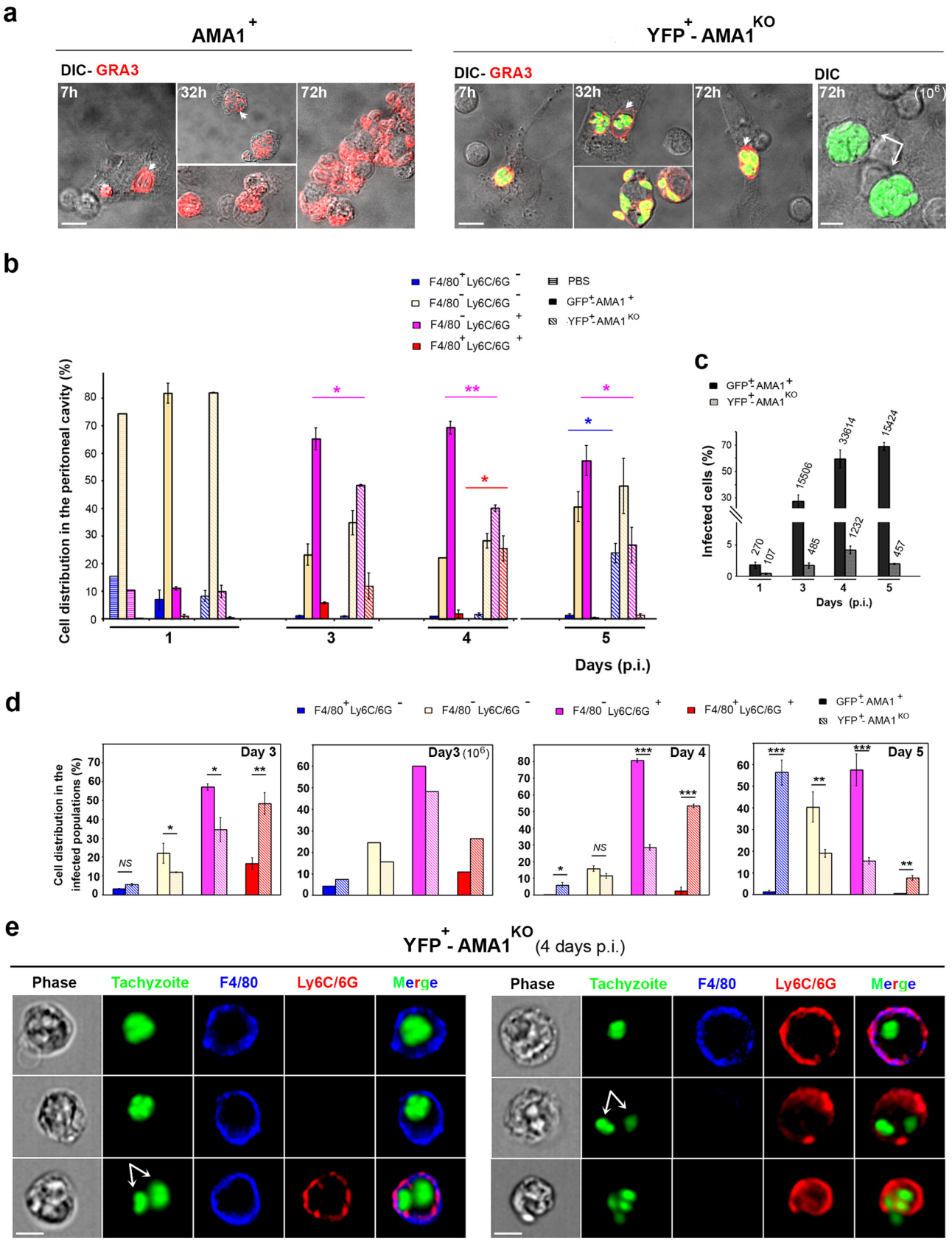

FIG 3 AMA1^{KO} and AMA1^{+} tachyzoites colonize resident and inflowing immune cells. (a) Cells from the peritoneal fluids of mice inoculated with 10^5 DiCre YFP^{-} AMA1^{+} (left panel) or 10^5 or 10^6 DiCre YFP^{+} AMA1^{KO} (right panel). The GRA3 protein was detected in growing parasites and in their surrounding PV/PVM (red; the white arrowheads point to the vacuoles, while white arrows point to the large vacuoles frequently seen with the 10^6 inoculum). (b to e) AMNIS analysis of cells from peritoneal exudates of mice inoculated with 10^5 GFP^{+} AMA1^{+} or YFP^{+} AMA1^{KO} and labeled for F4/80 and Ly6C/6G. (b) Relative distributions of cell subpopulations while mutant and wild-type tachyzoites are fluorescent. (c) Percentages of infected cells, with the numbers of cells analyzed indicated on top of each column. (d) Relative distributions between the infected cell subpopulations. (e) Images for each type of peritoneal cell infected by AMA1^{KO} parasites at day 4 p.i. Bars, 10 μM.

fected peritoneal cells were imaged by AMNIS, we detected the three leukocyte populations but we noticed that F4/80$^+$ Ly6C/6G$^+$ (GR1$^+$ inflammatory monocytes) as well as F4/80$^-$ Ly6C/6G$^+$ cells often carried distinct AMA1^{KO}-containing vacuoles, each likely to support parasite replication (Fig. 3e, white arrows). Of note, similar observations were also made for the AMA1$^+$-infected cells (Fig. 4a; the white arrows point to possibly distinct vacuoles). Finally, we could also detect Ly6C/6G$^+$ monocyte inside a F4/80$^+$ macrophage, indicating phagocytic uptake of AMA1$^+$-infected leukocytes (Fig. 4a, bottom panel).

Because the F4/80$^-$ and Ly6C/6G$^+$ leukocyte subsets include neutrophils, dendritic cells, and subpopulations of lymphocytes, we next used the Ly6G marker (clone 1A8) (41) to specifically discriminate neutrophils in the population of infected cells. Cell imaging revealed that both AMA1^{KO} (Fig. 4b, top panel) and AMA1$^+$ (Fig. 4b, bottom panel) tachyzoites were hosted in these F4/80$^-$ Ly6C/6G$^+$ Ly6G$^+$-positive cells, i.e., in neutrophils, where they likely multiply, considering the number of closely apposed individuals inside the cells (Fig. 4b, white arrows and arrowheads). In addition, AMNIS quantification revealed that the neutrophils constituted a substantial subset of the infected cells for both the mutant and the wild-type parasites, which, however, reached more than 40% for the latter and was thereby shown to be significantly higher than for the AMA1^{KO} parasites (Fig. 4c). Of note, the proportion of Ly6C/6G$^-$ Ly6G$^-$ hosting parasites was also important and significantly higher for the AMA1 mutant population, which is consistent with the quantification presented in Fig. 3d. Collectively, these data highlighted that both AMA1$^+$ and AMA1^{KO} parasites grew in resident and homing leukocytes at the site of inoculation and suggest subtle preferences for both Gr1$^+$ monocytes and macrophages in the leukocyte repertoire hosting the AMA1^{KO} over neutrophils, the latter being dominant in the case of AMA1$^+$ parasites.

Interestingly, despite the difference in the parasite loads, the replicative property of AMA1^{KO} seemed unaffected since statistically similar percentages of either single parasites or multiple (>2) parasites per cell characterized the AMA1$^+$-GFP and AMA1^{KO}-YFP-positive cells at day 4 p.i. (Fig. 4d). Finally, while the amounts of AMA1^{KO} tachyzoite-associated cells subsided over time to reach levels below 1% at days 8, 12, and 15 p.i. (data not shown), these were distributed equally between the F4/80$^+$ Ly6C/6G$^+$ inflammatory monocyte cell populations and the F4/80$^-$ Ly6C/6G$^+$ neutrophil cell populations (Fig. 4e, upper panel; the amounts of total peritoneal cells and of the infected subset analyzed by ImageStream are indicated on top of each column for each time point). Of note, these rare infected cells most often carried a single tachyzoite. Since most images showed round parasites (Fig. 4f, white arrowhead) inside F4/80$^-$ Ly6C/6G$^+$cells, with some being themselves engulfed in F4/80$^+$ cells (white arrow), this suggests that a macrophage phagocytic activity could contribute to the process of parasite clearance. Of note, because YFP fluorescence in phagosomes is pH and halide sensitive, while GFP fluorescence is only pH sensitive, the results of comparison of the *Toxoplasma* YFP$^+$-associated signal (AMA1^{KO}) to the GFP$^+$ signal (AMA1$^+$) could be slightly biased, as previously reported with other strains (21). However, the transient increase of the AMA1^{KO} parasite burden in the first days of infection and the observation of few cells positive for AMA1^{KO} round parasites at days 8, 12, and 15 p.i. in healthy mice, at times at which the mice infected with GFP$^+$-AMA1$^+$ had already succumbed, indicate that if there was an impact in fluorescence signals to measure parasite fate with time, it was minor. Finally, while specific *Toxoplasma* antibodies could act in concert with macrophages to control infection, we did not observe significant amounts of free AMA1^{KO} tachyzoites in peritoneal fluids from infected mice, regardless of the kinetics of infection, whereas exudates from AMA1$^+$-infected mice were commonly contaminated by free tachyzoites, in particular, from day 3 p.i. (data not shown). Accordingly, the reduction in the AMA1^{KO} parasite load observed over time correlated with the increase in time required for peritoneal cell samples to lyse an HFF monolayer in plaque assays and confirmed that most AMA1^{KO} parasites were cleared from the peritoneal cavity in less than 2 weeks (Fig. 4e, bottom panels).

AMA1^{KO} tachyzoites colonize mesothelial cells in the peritoneal tissue and expand massively in immunocompromised mice. We further analyzed whether mesothelial cells lining the serosal peritoneal cavity and in contact with the inoculum could also host parasites. Using a protocol that includes careful but extensive peritoneal washes to efficiently remove macrophages, monocytes, and lymphocytes, followed by a protease-directed digestion of the mesothelium that dissociates the constituting mesothelial cells (26), we analyzed at day 3 p.i. those that adhered, spread, and survived on gelatin-coated coverslips and found they were all F4/80$^-$, two criteria that distinguish mesothelial from hematopoietic cells. In addition, mouse mesothelial cells have been shown to express vimentin (Vim) and cytokeratin (CK) intermediate-filament (IF) proteins during short-term culture, the former taking over with time (26, 42–44). Among cells recovered from the mesothelium wall at day 3 p.i., 28% ± 5.2% cells were found positive for vimentin (Vim$^+$) whereas about 11.5% ± 2.8% were found positive for cytokeratin (CK$^+$) (n = 500 cells, triplicate, 1 experiment representative of 3 to 4 independent experiments with n = 2 different mice per strain) (Fig. 5). The other cells were negative for both IF markers, probably as a consequence of the network disassembly that occurs during cell cycle and senescence (45, 46). We detected AMA1^{KO} and AMA1$^+$ parasites within GRA3$^+$ vacuoles in the well-spread cells (Fig. 5, top panels, white arrows): after inoculation of 10^6 AMA1^{KO} tachyzoites, about 11% of the sampled mesothelial cells (n = 500 cells, triplicate for n = 2 mice) contained growing AMA1^{KO} parasites and 42% of these were expressing vimentin (n = 100 cells, triplicate for n = 2 mice) (Fig. 5, left bottom panel, white arrows). In parallel, in mesothelial cells collected from mice inoculated with 10^5 AMA1$^+$ tachyzoites, we found heavily Vim$^+$- or CK$^+$-infected cells together with large numbers of free parasites, an observation that fits with extensive tissue damage and parasite release (Fig. 5, right panels).

Importantly, when mice received the glucocorticoid dexamethasone that exerts anti-inflammatory and immunosuppressive effects (47) prior to receiving 10^5 AMA1^{KO} and thereafter, they failed to control parasite population expansion and died within 8 to 12 days, whereas the immunocompetent infected mice and the immunocompromised but noninfected counterparts all survived (1 experiment, n = 4 mice per group, data not shown). In immunocompromised mice, 22% ± 5.5% and 27% ± 3.8% mesothelial and peritoneal cells, respectively, permissive to parasite growth were detected as early as 2 days p.i. (n = 500 cells, duplicate experiments for n = 2 mice; see Fig. S2 in the supplemental material). These data document the mesothelium as permissive to both AMA1$^+$ and AMA1^{KO} tachyzoites, in the restricted context

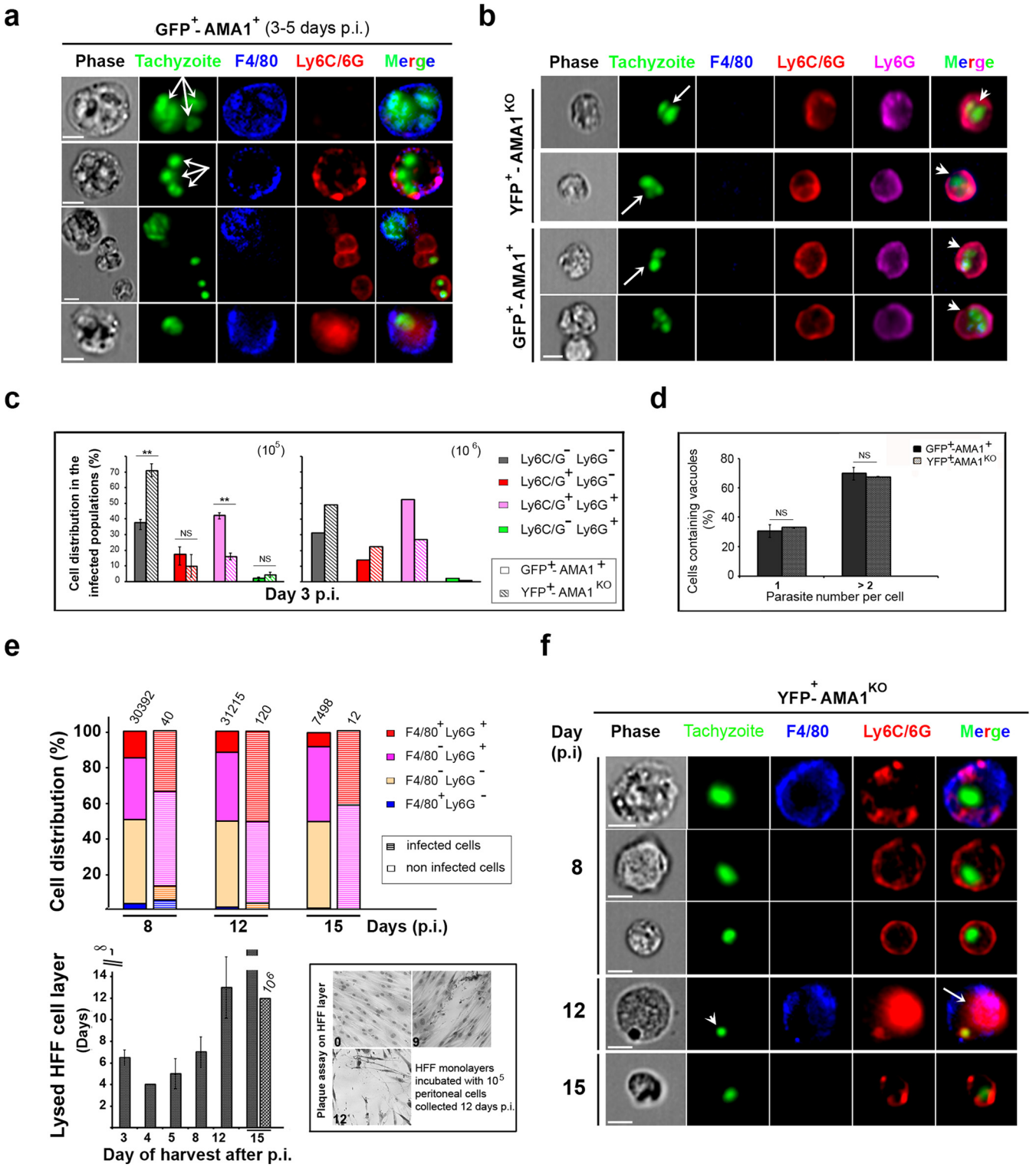

FIG 4 Neutrophils are hosting AMA1^{KO} and AMA1^{+} tachyzoites. (a, b, and f) AMNIS images of cells hosting GFP^{+}-AMA1^{+} tachyzoites (a and b) or YFP^{+}-AMA1^{KO} tachyzoites (b and f) at days 3 to 5 p.i. (a and b) and days 8, 12, and 15 p.i. (f). In panel a, the white arrows point to growing tachyzoites; in panel b, the white arrows (frames for green fluorescence) and arrowheads (merged frames) indicate the neutrophil (LY6G^{+}) subset hosting tachyzoites; in panel f, a single dying tachyzoite (white arrowhead) in an inflammatory monocyte (white arrow) is engulfed by a macrophage. (c, d, and e) Histograms showing the distributions of F4/80^{-} cell subpopulations hosting AMA1^{KO} and AMA1^{+} tachyzoites (c), infected cells carrying a single parasite or two or more parasites (d), and total peritoneal AMA1^{KO}-infected cell subpopulations at days 8, 12, and 15 p.i. (the amount of cells analyzed by AMNIS is indicated on top of each column) (e, top panel) and plaque assays on HFF monolayers (e, bottom panel). Histogram shows the average number of days required to fully lyse a HFF monolayer after addition of 10^5 peritoneal cells collected over time p.i. with AMA1^{KO} tachyzoites. Because no HFF lysis was observed when 10^5 peritoneal cells collected at day 15 p.i. were deposited (time to lyse infinite), we also incubated the HFF monolayer with 10^6 cells harvested at that latest time point p.i. The images (right frame) show the area of cell lysis increasing with culture time (days 9 and 12) when 10^5 peritoneal cells collected at day 12 p.i. were added to HFF monolayers. Bars, 10 μM.

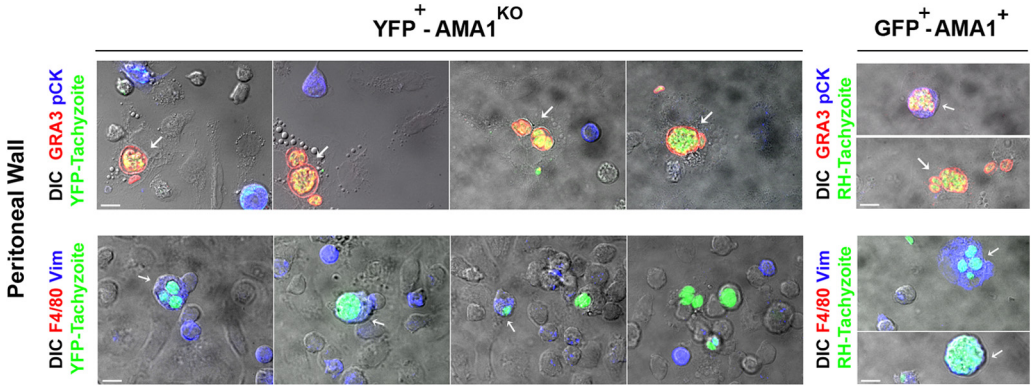

FIG 5 AMA1^{KO} tachyzoites massively colonize mesothelium. DIC-fluorescent merged images of cells released from the mesothelium of mice inoculated with YFP^{+}-AMA1^{KO} (left panels) and GFP^{+}-AMA1^{+} (right panels) tachyzoites were stained for F4/80 molecules (red, bottom panel) or cytokeratin (blue, top panel) or vimentin (blue, bottom panel) proteins; parasitophorous vacuoles and parasites were stained for GRA3 protein (red, top panel). The white arrows indicated the cells containing tachyzoites. Bars in all panels, 10 μM.

of the peritoneal route of infection. However, one could consider the contribution of mesothelial cells from other anatomical origins, including pleural and pericardial cells that are known to share structural and functional properties (44), in particular, during reactivation of the parasitic process from these corresponding organ reservoirs. Collectively, these results support the idea of a significant contribution of functional resident and homing leukocytes in the control of the AMA1^{KO} population.

Mice infected with AMA1^{KO} parasites seroconvert and are protected against secondary challenges. Since AMA1^{KO} parasites established only transiently in mice, we next investigated the immune status of these mice. First, in the BALB/c, C57BL/6J, and CD-1 mouse genotypes, we observed that most mouse sera contained anti-*Toxoplasma* antibodies (Fig. 6a; in the left panel, the doses of AMA1^{KO} inoculum are indicated on top of each lane; in the right panel, the number of mice serologically tested is indicated on top of each column). Second, we checked whether these mice were immunized against i.p. challenges with type I and II *Toxoplasma* strains. While BALB/c naive mice inoculated with 10^5 AMA1^{+} (type I) parasites died within 6 days, those that were initially injected with either 10^5 or 10^6 AMA1^{KO} parasites 8 to 10 weeks earlier survived the challenge over the assay period of 60 days (3 independent experiments for 10^5 parasites and 1 experiment for 10^6 parasites, $n = 5$ mice per dose and per assay) (Fig. 6b). The protection went down to 18% when a lower AMA1^{KO} dose (10^3 AMA1^{KO} parasites) was first injected (Fig. 6b, 2 independent experiments, $n = 5$ and 6 mice, respectively), which is consistent with the variable rate of seroconversion (Fig. 6a), and it was also reduced for the subcutaneous route of immunization (see Fig. S1b in the supplemental material). A rather long-lasting immunity was conferred to C57BL/6J mice immunized with 2.5×10^2 and 1.5×10^3 AMA1^{KO} tachyzoites and challenged 15 weeks later with the lethal dose of 10^3 AMA1^{+} tachyzoites (1 experiment, $n = 3$ mice per dose) (Fig. 6b, middle), while immunity lasting more than 8 months was mounted in BALB/c mice immunized with 10^5 AMA1^{KO} tachyzoites which resisted challenge with 10^5 virulent tachyzoites (1 experiment, $n = 7$ mice) (data not shown). Regarding the CD-1 mice, they also survived challenge with 10^5 AMA1^{+} tachyzoites when they were immunized with 10^4 or 10^6 AMA1^{KO} parasites (1 experiment, $n = 4$ mice per dose) (Fig. 6b). Finally, 60% of BALB/c mice immunized with 10^5 AMA1^{KO} parasites and challenged 8 weeks later with 10^3 type II ME49 tachyzoites gave negative results by qPCR for the presence of parasites in their brain whereas 100% of the nonimmunized mice gave positive results (1 assay, $n = 2$ and 5 for control and immunized mice, respectively) (Fig. 6c).

DISCUSSION

AMA1 is a protein that is structurally highly conserved across the Apicomplexa phylum (48), and *T. gondii* tachyzoites and *Plasmodium* merozoites lacking *AMA1* are significantly reduced in their invasive potential, unlike *Plasmodium* sporozoites, but the exact mechanism of the AMA1 contribution(s) to invasion remains a matter of debate (19, 49–51). We therefore asked whether AMA1 loss would affect the *Toxoplasma*-induced parasitic process in laboratory mice of different genotypes and, if so, what the consequences would be for the immune innate and adaptive responses triggered by the parasites.

We found that, in contrast to the AMA1-expressing tachyzoites, the uncontrolled development of which resulted in an uncontrolled and lethal inflammatory process, the AMA1^{KO} population did establish progenies within distinct cell lineages, but only transiently, and mice accordingly survived the infection. After i.p. inoculation of tachyzoites into BALB/c mice, the lack of AMA1 did not prevent the rapid colonization of (i) the mesothelial cells that line the peritoneal cavity wall, (ii) resident macrophages, and (iii) leukocytes recruited within this peritoneal environment, but the population declined, becoming undetectable after 2 weeks. AMA1^{KO} parasite clearance was ascertained as no signs of secondary toxoplasmosis were ever observed when inoculated mice received the immunosuppressive dexamethasone and no *T. gondii*-specific DNA was ever detected in brain of mice surviving the infection (see Fig. 3 in the supplemental material).

Of note, this report documents that *T. gondii* parasites infect mesothelial cells within few hours post-parasite delivery in the peritoneal cavity, and this held true for both the AMA1^{+} and AMA1^{KO} parasite strains. Because these cells sense and respond to signals within their tissue milieu, they play central roles in peritoneal homeostasis and inflammation by producing multiple mediators, including CCL2, IL-6, and TNF-α cytokines (43, 44, 52). Therefore, their early interaction with tachyzoites expressing or not expressing AMA1 is likely to initiate and contribute to the

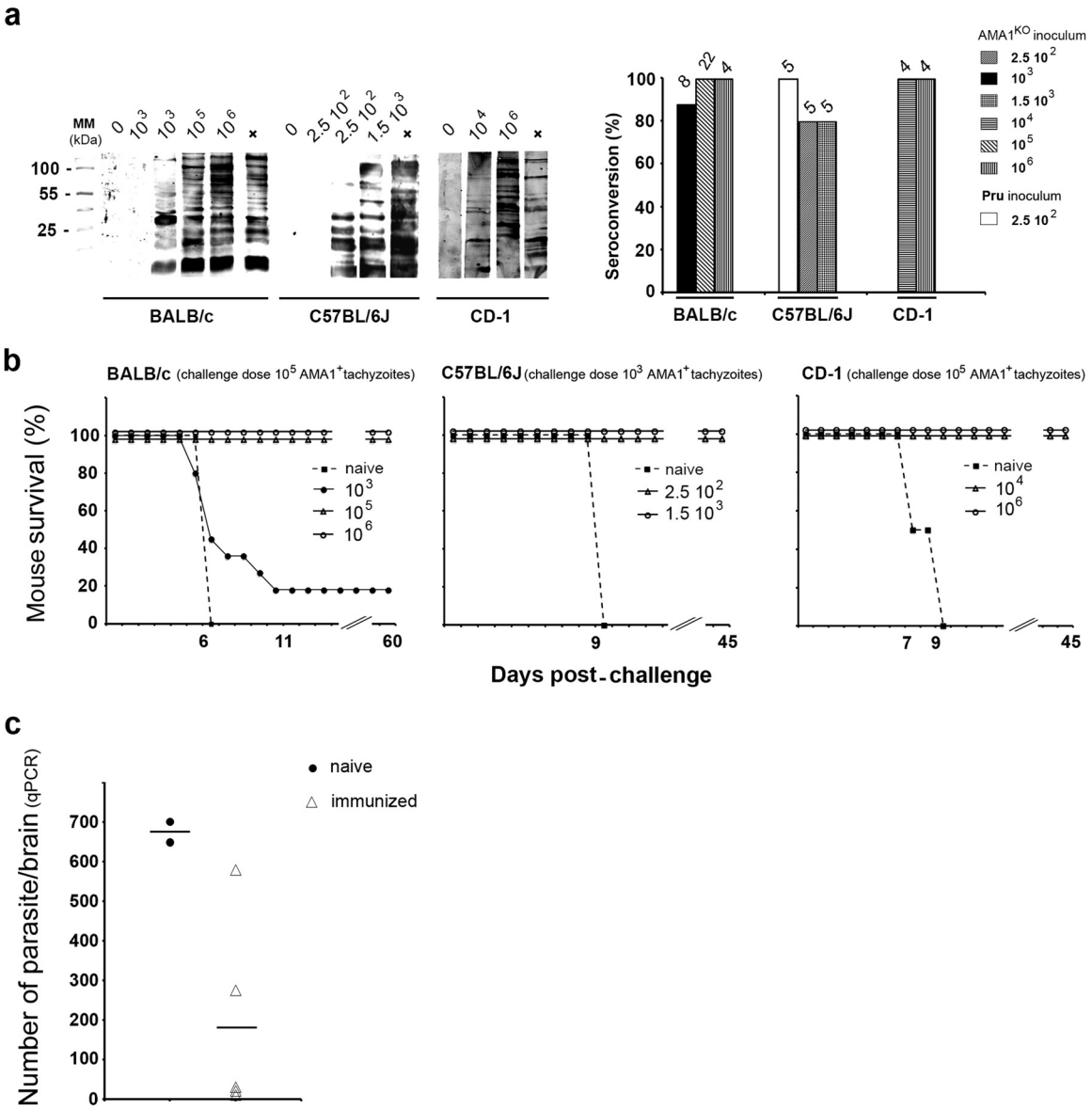

FIG 6 Mice infected with AMA1^{KO} parasites seroconvert and are protected against new infections. (a) (Left panel) Reactivity of sera from AMA1^{KO}-inoculated mice 6 to 8 weeks p.i. Western blots show results from 1 representative mouse for each dose of AMA1^{KO} parasites injected. The inoculation doses are indicated on top of each lane: 0 and + refer to the reactivity of sera from a naive mouse and a mouse infected with the cystogenic type II PruΔ*KU80* strain, respectively. (Right panel) Histogram showing the rate of seroconversion of mice. The number of mice analyzed is indicated on top of each column. (b) Mouse survival curves after immunization with different doses of AMA1^{KO} tachyzoites and challenges with various amounts of type I virulent AMA1^{+} tachyzoites. The numbers indicated in the graphs are the inoculum doses at which mice survived. The mice were then challenged with 10^5 AMA1^{+} parasites for BALB/c and CD1 mice and 10^3 AMA1^{+} parasites for C57BL6 mice. (c) Parasite burden in the brain of infected BALB/c mice challenged ($n = 5$) or not ($n = 2$) by AMA1^{KO} parasites and then i.p. injected with 10^3 type II (ME49) tachyzoites 8 weeks later. A *T. gondii* RT-PCR assay was performed on brain tissue extracts 6 weeks postinfection, and data are calibrated with known numbers of parasites.

signaling cascades typifying the immune processes. *In situ* ImageStream analysis revealed that during the transient phase of expansion, AMA1^{KO} tachyzoites invaded and multiplied in various leukocytes but preferentially in the Gr1^{+} monocyte homing subset. Interestingly, the frequency of cells harboring two or more vacuoles was surprisingly high whereas the global level of cell infection remained low, thus possibly reflecting selective phagocytosis of infected cells by other infected cells. On the other hand, a few images, in particular, those corresponding to the period when the population started to decline, showed that both the monocytes and neutrophils that were associated with single and/or abnormally shaped parasites could be engulfed in macrophages, pointing to a process of clearance of parasites and hosting cells. Importantly, when the mouse immune responses were compromised prior to inoculation and thereafter, the AMA1^{KO} population rapidly and extensively expanded throughout tissues and eventually killed the host, thereby demonstrating that the AMA1^{KO} tachyzoites had retained intrinsic infectious capabilities.

However, the rapid control of the AMA1^{KO} population in im-

munocompetent mice was clearly associated with a lower overall capacity of these mutants to proliferate. Since the replicative potential *per se* of the zoites seemed unaffected within the early phase of parasitism, an overall deficiency in invasiveness compared to that of the AMA1^{+} population is plausible, and this observation recalls what has been described under *in vitro* conditions. There is, however, no way to precisely assess *in vivo* at which preinvasive or invasive step AMA1^{KO} tachyzoites are deficient. Interestingly, despite the expression of AMA1 homologues that has been acknowledged in several AMA1^{KO} lines (19, 50), the *in vivo* phenotype of AMA1^{KO} parasites has remained stable over the years of study and can be complemented only under conditions of expression of an exogenous copy of *AMA1* (AMA1^{FLAG} strain). More specifically, the outcome of the inoculation of AMA1^{KO} parasites in mice did not vary within the 2-year study despite long-term *in vitro* parasite culture. While a modest gain in *in vitro* invasiveness of the AMA1^{KO} tachyzoites over 12 months of culture has been recently assigned to the expression of AMA1 homologues (50), the AMA1^{KO} line which expresses AMA1 homologues (19) remained impaired in fitness, consistent with a quite minor compensation for loss of AMA1 that remains inefficient at restoring the overall expansion potential of the parasite population in its host. Interestingly, the results of our study are also in line with the idea that the invasive capability of the zoite crucially determines the population fate *in vivo*, thereby validating the interest in designing anti-invasive strategies for intervention against apicomplexan parasites.

Since the AMA1^{KO}-driven immune processes promoted seroconversion, we also tested whether mice were immunized against secondary challenges with different *T. gondii* strains. We report full and lasting protection against a high inoculum of the lethal type I strain in the 3 mouse genotypes tested when AMA1^{KO} tachyzoites were initially delivered i.p. and a more variable protection after a primary challenge delivered subcutaneously. Importantly, after the secondary challenge with the cystogenic type II ME49 strain, we noticed a lower level of parasitism in the mouse brains.

In conclusion, this work demonstrates that a lack of AMA1 does not prevent host cell infection within distinct host cell subsets in laboratory mice. The early innate immune response elicited by the parasitism implicates short-term and moderate secretion of proinflammatory cytokines and further proceeds to an immune status protective against reinfection. However, whether the defect in the virulence of the AMA1-deficient strain results not only from the reduction of AMA1^{-} parasite invasiveness but also from an increased immune control of AMA1^{-} parasites remains to be addressed. Future studies might then bring valuable insights into how the host immune system senses and processes early phases of parasitism to design efficient strategies against adverse effects of parasite persistence, or against acute primary toxoplasmosis, which is now also diagnosed in immunocompetent humans (53). This work should also pave the way for further investigations of the vaccinal properties of AMA1-deficient zoites of other economically important Apicomplexa parasites.

ACKNOWLEDGMENTS

We are grateful to G. Ward (University of Vermont, VT, USA) and V. Carruthers (University of Ann Arbor, MI, USA) for providing us with the anti-AMA1 and anti-M2AP antibodies, respectively. We thank the Center for Human Immunology at Institut Pasteur (Paris, France) for support using the ImageStream AMNIS.

REFERENCES

1. **Thompson RC, Kutz SJ, Smith A.** 2009. Parasite zoonoses and wildlife: emerging issues. Int J Environ Res Public Health **6:**678–693. http://dx.doi.org/10.3390/ijerph6020678.
2. **Hill DE, Dubey JP.** 2013. Toxoplasma gondii prevalence in farm animals in the United States. Int J Parasitol **43:**107–113. http://dx.doi.org/10.1016/j.ijpara.2012.09.012.
3. **Pappas G, Roussos N, Falagas ME.** 2009. Toxoplasmosis snapshots: global status of Toxoplasma gondii seroprevalence and implications for pregnancy and congenital toxoplasmosis. Int J Parasitol **39:**1385–1394. http://dx.doi.org/10.1016/j.ijpara.2009.04.003.
4. **Montoya JG, Liesenfeld O.** 2004. Toxoplasmosis. Lancet **363:**1965–1976. http://dx.doi.org/10.1016/S0140-6736(04)16412-X.
5. **Su C, Khan A, Zhou P, Majumdar D, Ajzenberg D, Dardé ML, Zhu XQ, Ajioka JW, Rosenthal BM, Dubey JP, Sibley LD.** 2012. Globally diverse Toxoplasma gondii isolates comprise six major clades originating from a small number of distinct ancestral lineages. Proc Natl Acad Sci U S A **109:**5844–5849. http://dx.doi.org/10.1073/pnas.1203190109.
6. **Yang N, Farrell A, Niedelman W, Melo M, Lu D, Julien L, Marth GT, Gubbels MJ, Saeij JP.** 2013. Genetic basis for phenotypic differences between different Toxoplasma gondii type I strains. BMC Genomics **14:**467–486. http://dx.doi.org/10.1186/1471-2164-14-467.
7. **Lilue J, Müller UB, Steinfeldt T, Howard JC.** 2013. Reciprocal virulence and resistance polymorphism in the relationship between Toxoplasma gondii and the house mouse. Elife **2:**e01298. http://dx.doi.org/10.7554/eLife.01298.
8. **Khan A, Behnke MS, Dunay IR, White MW, Sibley LD.** 2009. Phenotypic and gene expression changes among clonal type I strains of Toxoplasma gondii. Eukaryot Cell **8:**1828–1836. http://dx.doi.org/10.1128/EC.00150-09.
9. **Jongert E, Roberts CW, Gargano N, Förster-Waldl E, Petersen E.** 2009. Vaccines against Toxoplasma gondii: challenges and opportunities. Mem Inst Oswaldo Cruz **104:**252–266. http://dx.doi.org/10.1590/S0074-02762009000200019.
10. **Liu Q, Singla LD, Zhou H.** 2012. Vaccines against Toxoplasma gondii: status, challenges and future directions. Hum Vaccin Immunother **8:**1305–1308. http://dx.doi.org/10.4161/hv.21006.
11. **Cérède O, Dubremetz J, Soête M, Deslée D, Vial H, Bout D, Lebrun M.** 2005. Synergistic role of micronemal proteins in Toxoplasma gondii virulence. J Exp Med **201:**453–463. http://dx.doi.org/10.1084/jem.20041672.
12. **Mévélec M, Ducournau C, Bassuny Ismael A, Olivier M, Sèche E, Lebrun M, Bout D, Dimier-Poisson I.** 2010. Mic1-3 knockout Toxoplasma gondii is a good candidate for a vaccine against T. gondii-induced abortion in sheep. Vet Res **41:**49. http://dx.doi.org/10.1051/vetres/2010021.
13. **Fox BA, Bzik DJ.** 2002. De novo pyrimidine biosynthesis is required for virulence of Toxoplasma gondii. Nature **415:**926–929. http://dx.doi.org/10.1038/415926a.
14. **Fox BA, Bzik DJ.** 2010. Avirulent uracil auxotrophs based on disruption of orotidine-5′-monophosphate decarboxylase elicit protective immunity to Toxoplasma gondii. Infect Immun **78:**3744–3752. http://dx.doi.org/10.1128/IAI.00287-10.
15. **Baird JR, Fox BA, Sanders KL, Lizotte PH, Cubillos-Ruiz JR, Scarlett UK, Rutkowski MR, Conejo-Garcia JR, Fiering S, Bzik DJ.** 2013. Avirulent Toxoplasma gondii generates therapeutic antitumor immunity by reversing immunosuppression in the ovarian cancer microenvironment. Cancer Res **73:**3842–3851. http://dx.doi.org/10.1158/0008-5472.CAN-12-1974.
16. **Baird JR, Byrne KT, Lizotte PH, Toraya-Brown S, Scarlett UK, Alexander MP, Sheen MR, Fox BA, Bzik DJ, Bosenberg M, Mullins DW, Turk MJ, Fiering S.** 2013. Immune-mediated regression of established B16F10 melanoma by intratumoral injection of attenuated Toxoplasma gondii protects against rechallenge. J Immunol **190:**469–478. http://dx.doi.org/10.4049/jimmunol.1201209.
17. **Innes EA, Bartley PM, Maley S, Katzer F, Buxton D.** 2009. Veterinary vaccines against Toxoplasma gondii. Mem Inst Oswaldo Cruz **104:**246–251. http://dx.doi.org/10.1590/S0074-02762009000900031.
18. **Hill RD, Gouffon JS, Saxton AM, Su C.** 2012. Differential gene expression in mice infected with distinct Toxoplasma strains. Infect Immun **80:**968–974. http://dx.doi.org/10.1128/IAI.05421-11.

19. **Bargieri DY, Andenmatten N, Lagal V, Thiberge S, Whitelaw JA, Tardieux I, Meissner M, Ménard R.** 2013. Apical membrane antigen 1 mediates apicomplexan parasite attachment but is dispensable for host cell invasion. Nat Commun **4:**2552. http://dx.doi.org/10.1038/ncomms3552.
20. **Donahue CG, Carruthers VB, Gilk SD, Ward GE.** 2000. The Toxoplasma homolog of Plasmodium apical membrane antigen-1 (AMA-1) is a microneme protein secreted in response to elevated intracellular calcium levels. Mol Biochem Parasitol **111:**15–30. http://dx.doi.org/10.1016/S0166-6851(00)00289-9.
21. **Dupont CD, Christian DA, Selleck EM, Pepper M, Leney-Greene M, Harms Pritchard G, Koshy AA, Wagage S, Reuter MA, Sibley LD, Betts MR, Hunter CA.** 2014. Parasite fate and involvement of infected cells in the induction of CD4+ and CD8+ T cell responses to Toxoplasma gondii. PLoS Pathog **10:**e1004047. http://dx.doi.org/10.1371/journal.ppat.1004047.
22. **Fox BA, Falla A, Rommereim LM, Tomita T, Gigley JP, Mercier C, Cesbron-Delauw MF, Weiss LM, Bzik DJ.** 2011. Type II Toxoplasma gondii KU80 knockout strains enable functional analysis of genes required for cyst development and latent infection. Eukaryot Cell **10:**1193–1206. http://dx.doi.org/10.1128/EC.00297-10.
23. **Andenmatten N, Egarter S, Jackson AJ, Jullien N, Herman JP, Meissner M.** 2013. Conditional genome engineering in Toxoplasma gondii uncovers alternative invasion mechanisms. Nat Methods **10:**125–127. http://dx.doi.org/10.1038/nmeth.2301.
24. **Gonzalez V, Combe A, David V, Malmquist NA, Delorme V, Leroy C, Blazquez S, Ménard R, Tardieux I.** 2009. Host cell entry by apicomplexa parasites requires actin polymerization in the host cell. Cell Host Microbe **5:**259–272. http://dx.doi.org/10.1016/j.chom.2009.01.011.
25. **Nicoll S, Wright S, Maley SW, Burns S, Buxton D.** 1997. A mouse model of recrudescence of Toxoplasma gondii infection. J Med Microbiol **46:**263–266. http://dx.doi.org/10.1099/00222615-46-3-263.
26. **Bot J, Whitaker D, Vivian J, Lake R, Yao V, McCauley R.** 2003. Culturing mouse peritoneal mesothelial cells. Pathol Res Pract **199:**341–314. http://dx.doi.org/10.1078/0344-0338-00427.
27. **Rabenau KE, Sohrabi A, Tripathy A, Reitter C, Ajioka JW, Tomley FM, Carruthers VB.** 2001. TgM2AP participates in Toxoplasma gondii invasion of host cells and is tightly associated with the adhesive protein TgMIC2. Mol Microbiol **41:**537–547. http://dx.doi.org/10.1046/j.1365-2958.2001.02513.x.
28. **Schneider CA, Rasband WS, Eliceiri KW.** 2012. NIH Image to ImageJ: 25 years of image analysis. Nat Methods **9:**671–675. http://dx.doi.org/10.1038/nmeth.2089.
29. **Delorme-Walker V, Abrivard M, Lagal V, Anderson K, Perazzi A, Gonzalez V, Page C, Chauvet J, Ochoa W, Volkmann N, Hanein D, Tardieux I.** 2012. Toxofilin upregulates the host cortical actin cytoskeleton dynamics, facilitating Toxoplasma invasion. J Cell Sci **125:**4333–4342. http://dx.doi.org/10.1242/jcs.103648.
30. **Reischl U, Bretagne S, Krüger D, Ernault P, Costa JM.** 2003. Comparison of two DNA targets for the diagnosis of Toxoplasmosis by real-time PCR using fluorescence resonance energy transfer hybridization probes. BMC Infect Dis **3:**7. http://dx.doi.org/10.1186/1471-2334-3-7.
31. **Cannella D, Brenier-Pinchart MP, Braun L, van Rooyen JM, Bougdour A, Bastien O, Behnke MS, Curt RL, Curt A, Saeij JPJ, Sibley LD, Pelloux H, Hakimi MH.** 27 February 2014, posting date. miR-146a and miR-155 delineate a microRNA fingerprint associated with Toxoplasma persistence in the host brain. Cell Rep http://dx.doi.org/10.1016/j.celrep.2014.02.002.
32. **Aldinger KA, Sokoloff G, Rosenberg DM, Palmer AA, Millen KJ.** 2009. Genetic variation and population substructure in outbred CD-1 mice: implications for genome-wide association studies. PLoS One **4:**e4729. http://dx.doi.org/10.1371/journal.pone.0004729.
33. **Mordue DG, Sibley LD.** 2003. A novel population of Gr-1+-activated macrophages induced during acute toxoplasmosis. J Leukoc Biol **74:**1015–1025. http://dx.doi.org/10.1189/jlb.0403164.
34. **Alexander J, Scharton-Kersten TM, Yap G, Roberts CW, Liew FY, Sher A.** 1997. Mechanisms of innate resistance to Toxoplasma gondii infection. Philos Trans R Soc Lond B Biol Sci **352:**1355–1359. http://dx.doi.org/10.1098/rstb.1997.0120.
35. **Robben PM, LaRegina M, Kuziel WA, Sibley LD.** 2005. Recruitment of Gr-1+ monocytes is essential for control of acute toxoplasmosis. J Exp Med **201:**1761–1769. http://dx.doi.org/10.1084/jem.20050054.
36. **Dunay IR, Fuchs A, Sibley LD.** 2010. Inflammatory monocytes but not neutrophils are necessary to control infection with Toxoplasma gondii in mice. Infect Immun **78:**1564–1570. http://dx.doi.org/10.1128/IAI.00472-09.
37. **Howard J, Hunn J, Steinfeldt T.** 2011. The IRG protein-based resistance mechanism in mice and its relation to virulence in Toxoplasma gondii. Curr Opin Microbiol **14:**414–421. http://dx.doi.org/10.1016/j.mib.2011.07.002.
38. **Etheridge RD, Alaganan A, Tang K, Lou HJ, Turk BE, Sibley LD.** 2014. The Toxoplasma pseudokinase ROP5 forms complexes with ROP18 and ROP17 kinases that synergize to control acute virulence in mice. Cell Host Microbe **15:**537–550. http://dx.doi.org/10.1016/j.chom.2014.04.002.
39. **Achbarou A, Mercereau-Puijalon O, Sadak A, Fortier B, Leriche MA, Camus D, Dubremetz JF.** 1991. Differential targeting of dense granule proteins in the parasitophorous vacuole of Toxoplasma gondii. Parasitology **103:**321–329. http://dx.doi.org/10.1017/S0031182000059837.
40. **Geissmann F, Auffray C, Palframan R, Wirrig C, Ciocca A, Campisi L, Narni-Mancinelli E, Lauvau G.** 2008. Blood monocytes: distinct subsets, how they relate to dendritic cells, and their possible roles in the regulation of T-cell responses. Immunol Cell Biol **86:**398–408. http://dx.doi.org/10.1038/icb.2008.19.
41. **Daley JM, Thomay AA, Connolly MD, Reichner JS, Albina JE.** 2008. Use of Ly6G-specific monoclonal antibody to deplete neutrophils in mice. J Leukoc Biol **83:**64–70.
42. **Connell ND, Rheinwald JG.** 1983. Regulation of the cytoskeleton in mesothelial cells: reversible loss of keratin and increase in vimentin during rapid growth in culture. Cell **34:**245–253. http://dx.doi.org/10.1016/0092-8674(83)90155-1.
43. **Mutsaers SE, Wilkosz S.** 2007. Structure and function of mesothelial cells. Cancer Treat Res **134:**1–19.
44. **Yung S, Li FK, Chan TM.** 2006. Peritoneal mesothelial cell culture and biology. Perit Dial Int **26:**162–173.
45. **Chou YH, Rosevear E, Goldman RD.** 1989. Phosphorylation and disassembly of intermediate filaments in mitotic cells. Proc Natl Acad Sci U S A **86:**1885–1889. http://dx.doi.org/10.1073/pnas.86.6.1885.
46. **Goto H, Inagaki M.** 23 March 2014, posting date. New insights into roles of intermediate filament phosphorylation and progeria pathogenesis. IUBMB Life http://dx.doi.org/10.1002/iub.1260.
47. **Coutinho AE, Chapman KE.** 2011. The anti-inflammatory and immunosuppressive effects of glucocorticoids, recent developments and mechanistic insights. Mol Cell Endocrinol **335:**2–13. http://dx.doi.org/10.1016/j.mce.2010.04.005.
48. **Chesne-Seck ML, Pizarro JC, Vulliez-Le Normand B, Collins CR, Blackman MJ, Faber BW, Remarque EJ, Kocken CH, Thomas AW, Bentley GA.** 2005. Structural comparison of apical membrane antigen 1 orthologues and paralogues in apicomplexan parasites. Mol Biochem Parasitol **144:**55–67. http://dx.doi.org/10.1016/j.molbiopara.2005.07.007.
49. **Bargieri D, Lagal V, Andenmatten N, Tardieux I, Meissner M, Ménard R.** 2014. Host cell invasion by apicomplexan parasites: the junction conundrum. PLoS Pathog **10:**e1004273. http://dx.doi.org/10.1371/journal.ppat.1004273.
50. **Lamarque M, Roques M, Kong-Hap M, Tonkin M, Rugarabamu G, Marq J, Penarete-Vargas D, Boulanger M, Soldati-Favre D, Lebrun M.** 2014. Plasticity and redundancy among AMA-RON pairs ensure host cell entry of Toxoplasma parasites. Nat Commun **5:**4098. http://dx.doi.org/10.1038/ncomms5098.
51. **Yap A, Azevedo MF, Gilson PR, Weiss GE, O'Neill MT, Wilson DW, Crabb BS, Cowman AF.** 2014. Conditional expression of apical membrane antigen 1 in Plasmodium falciparum shows it is required for erythrocyte invasion by merozoites. Cell Microbiol **16:**642–656. http://dx.doi.org/10.1111/cmi.12287.
52. **Valle MT, Degl'Innocenti ML, Bertelli R, Facchetti P, Perfumo F, Fenoglio D, Kunkl A, Gusmano R, Manca F.** 1995. Antigen-presenting function of human peritoneum mesothelial cells. Clin Exp Immunol **101:**172–176.
53. **Dardé ML.** 2008. Toxoplasma gondii, "new" genotypes and virulence. Parasite **15:**366–371. http://dx.doi.org/10.1051/parasite/2008153366.